Heat flux for many-body interactions: Corrections to LAMMPS

Paul Boone[a], Hasan Babaei[a,b], and Christopher E. Wilmer[a]*

[a]Department of Chemical and Petroleum Engineering, University of Pittsburgh, Pittsburgh, Pennsylvania

[b]Department of Chemistry, University of California, Berkeley, California

* to whom correspondence should be addressed: wilmer@pitt.edu

Abstract

The virial stress tensor-based instantaneous heat flux, which is used by LAMMPS, is only valid for the small subset of simulations that contain only pairwise interactions. For systems that contain many-body interactions using 3- or 4-body potentials, a more complete derivation is required. We have created a software patch to LAMMPS that implements the correct heat flux calculation approach for 3- and 4-body potentials, based on the derivation by Torii et al[1]. Using two example systems, the error in the uncorrected code for many-body potential heat flux is shown to be significant and reaches nearly 100% of the many-body potential heat flux for the systems we studied; hence, the error of the total heat flux calculation is proportional to the fraction of the total heat flux transferred through the many-body potentials. This error may have consequences for calculating thermal conductivities calculated using the Green-Kubo method or any NEMD method that uses the instantaneous heat flux. We recommend that all researchers using LAMMPS for heat flux calculations where significant heat is transferred via the many-body potentials adopt the corrected code.

Introduction

LAMMPS is a commonly-used open-source molecular dynamics package[2] and can be used for, among other things, calculating thermal transport properties such as the thermal conductivity.[3–6] There are four common methods in LAMMPS to measure the thermal conductivity. Three of these are based on non-equilibrium molecular dynamics (NEMD), briefly: (1) enforcing a temperature gradient by thermostatting two regions and measuring the molecular heat flux or keeping track of the energy added and removed from the thermostatted regions,[7] (2) enforcing an energy flux by adding and removing a constant amount of energy to two defined regions and then measuring the resulting temperature gradient,[8] and (3) defining two regions and swapping the kinetic energy of atoms between the two regions to create a very small temperature gradient, and then measuring the exchanged energy (i.e. the Muller-Plathe method[9]). The fourth approach is the Green-Kubo method,[10,11] which uses the autocorrelation function of the instantaneous heat flux to calculate the thermal conductivity, under equilibrium conditions. In this paper, we describe an error with how LAMMPS calculates the instantaneous heat flux, which could affect thermal conductivity calculations that employ the instantaneous heat flux, such as some NEMD calculations (subset of case 1 above) as well as the Green-Kubo method. In general, this error will affect any calculation that employs the instantaneous heat flux, such as the calculation of per-potential heat fluxes.[12,13]

In LAMMPS, the function that calculates the instantaneous heat flux uses a virial stress tensor form. To the best of our knowledge, a derivation for this form of the heat flux has not been published, besides the terse form that exists in the LAMMPS documentation[14]. In systems involving only two-body potentials, this form is valid, but it cannot be extended to systems with many-body potentials. Torii et al[1] derive general expressions for many-body heat fluxes (which we will review below in the background section) but do not address differences with the virial stress tensor formulation. Fan et al[15] states that the LAMMPS virial stress heat flux applies only to two-body potentials, but does not go into detail about the derivation error in the stress-based form. Additionally, neither paper provides source code corrections to LAMMPS, although Fan et al does have an alternative GPU code available on request which is limited to specific potentials (the Stillinger-Weber and Tersoff potentials as currently publicized).

The purpose of this paper is three-fold: (1) to show how the virial stress tensor formulation used by LAMMPS to calculate heat flux is derived and how it compares to a correctly derived many-body heat flux, (2) to publish publicly-available code for correctly calculating many-body heat flux to LAMMPS, and (3) to demonstrate its importance using different example systems. We analyze an idealized metal-organic framework (MOF) where heat is transferred predominantly via the bond and angle potentials, and the liquid-phase hydrocarbons propane, octane, and hexadecane with bond, angle, dihedral and improper potentials. The scale of the error in the heat flux ranges from significant to inconsequential, depending on the system and how much of the heat flux transfers through the many-body potentials. The magnitude of this effect on thermal conductivities calculated via the Green Kubo method is difficult to generalize and is likely system dependent. The hydrocarbon system is particularly illustrative of the range of error and how the distribution of the heat flux through different potentials affects the total error in the system.

Background

In LAMMPS, the heat flux is calculated using a virial stress tensor form defined per atom. This definition, when appropriately limited to only two-body potentials, is provably equivalent to the Irving and Kirkwood[16] or Hardy[17] heat fluxes. In this section, we will show a complete derivation of a general heat flux expression for a many-body potential based on the derivation in Torii, et al.[1], before applying it to two-body potentials only in order to derive the virial stress tensor form of the heat flux used in LAMMPS. We can then compare the virial stress tensor as defined for many-body heat fluxes to our general derivation to see that the per atom virial stress tensor heat flux defined in LAMMPS is not a valid expression for the heat flux.

We start with the definitions of the instantaneous heat flux $\boldsymbol{J}$ and per-atom energy E_i:[18]

$$E_i = \frac{1}{2} m_i \boldsymbol{v}_i^2 + U_i \tag{1}$$

$$\begin{aligned} \boldsymbol{J}V &= \frac{d}{dt} \sum_i \boldsymbol{r}_i E_i \\ &= \sum_i E_i \boldsymbol{v}_i + \sum_i \boldsymbol{r}_i \frac{d}{dt} E_i \end{aligned} \tag{2-3}$$

Where V is the volume, and m_i, v_i, U_i, and $\boldsymbol{r}_i$ are the mass, velocity, potential energy, and position of the i^{th} atom. We can separate equation (3) into a convective term $\boldsymbol{J}_{cnv} = \sum_i E_i \boldsymbol{v}_i$ and a potential term $\boldsymbol{J}_{pot} = \sum_i \boldsymbol{r}_i \frac{d}{dt} E_i$ where $\boldsymbol{J}_{cnv}$ represents the heat flux due to the movement of atoms in the system, and $\boldsymbol{J}_{pot}$ represents the heat flux due to changes in atom potentials. Note that $\boldsymbol{J}_{cnv}$ is still dependent on the form of the atom potential U_i, which will in general involve a summation over all the potentials defined on the system; in this case: two-body, three-body, and four-body potentials. Here we define, $\mathbb{P}$, as the set all potentials $\mathbb{P} = \mathbb{P}_2 + \mathbb{P}_3 + \cdots + \mathbb{P}_m$ defined on the system, where $\mathbb{P}_2$ is all two-body potentials, $\mathbb{P}_3$ is all 3-body potentials, and $\mathbb{P}_{\text{m}}$ is all m-body potentials. Further, let $\mathbb{P}_{\text{mi}}$ refer to the set of all m-body potentials which include the atom i, and let U_ϕ be the potential energy for the specific potential ϕ. If we are looking at only two-, three- and four-body potentials, U_i can now be defined as:

$$U_i = \sum_{m=2}^{4} \sum_{\phi \in \mathbb{P}_{mi}} \frac{1}{m} U_\phi \tag{4}$$

Here, the total potential energy of atom i is the sum of all potentials that include the atom i divided by the number of atoms in each potential. In this way, the energy of each m-body potential is evenly divided up amongst the atoms that constitute it. There are other ways of distributing the potential energy between atoms but this does not affect the resulting aggregate heat flux.[1,18] We are evenly distributing them in this derivation for simplicity (and

because this is what LAMMPS does); interested readers can see a full derivation with arbitrarily distributed potential energies in the paper by Torii, et al.[1]

We have three definitions for forces: (1): let $\boldsymbol{F}_i$ be the sum of all forces on i, (2) let $\boldsymbol{F}_{i\phi}$ be the force on atom i due to a specific potential $\phi \in \mathbb{P}$, and (3) let $\boldsymbol{F}_{ij,\phi}$ be the force on atom i due to atom j as part of a specific potential $\phi \in \mathbb{P}$.

Expanding the $\boldsymbol{J}_{pot}$ term:

$$\begin{aligned}
\boldsymbol{J}_{pot} &= \sum_i \boldsymbol{r}_i \frac{d}{dt} E_i \\
&= \sum_i \boldsymbol{r}_i \frac{d}{dt}\left(\frac{1}{2} m_i \boldsymbol{v}_i^2 + U_i\right) \\
&= \sum_i \boldsymbol{r}_i (m_i \boldsymbol{a}_i \cdot \boldsymbol{v}_i) + \sum_i \boldsymbol{r}_i \frac{d}{dt}\left(\sum_{m=2}^{4} \sum_{\phi \in \mathbb{P}_{mi}} \frac{1}{m} U_\phi\right) \\
&= \sum_i \boldsymbol{r}_i (\boldsymbol{F}_i \cdot \boldsymbol{v}_i) + \sum_i \boldsymbol{r}_i \left(\sum_{m=2}^{4} \sum_{\phi \in \mathbb{P}_{mi}} \frac{1}{m} \frac{dU_\phi}{dt}\right) \qquad (5abcd)
\end{aligned}$$

To finish our definition of the $\boldsymbol{J}_{pot}$ term, we introduce some additional notation. First, we define $\boldsymbol{r}_{jk} = \boldsymbol{r}_j - \boldsymbol{r}_k$. We will also use the notation $j \in \phi$ to mean j is one of the atoms that constitutes the potential ϕ, and if we take all possible pairs of the atoms in ϕ, denoted $[\phi]^2$, then $\{j,k\} \in [\phi]^2$ will mean that $\{j,k\}$ is one of these pairs (e.g., for a two-, three- or four-body potential, there will be 1, 3, and 6 pairs, respectively). We also need to express the derivative dU_ϕ/dt in terms of the forces and velocities of its constituent atoms, where $r_j = |\boldsymbol{r}_j|$:

$$\frac{dU_\phi}{dt} = \sum_{j \in \phi} \frac{dU_\phi}{dr_j} \frac{dr_j}{dt} = -\sum_{j \in \phi} \boldsymbol{F}_{j\phi} \cdot \boldsymbol{v}_j \qquad (6)$$

Now:

$$\begin{aligned}
\boldsymbol{J}_{pot} &= \sum_i \boldsymbol{r}_i (\boldsymbol{F}_i \cdot \boldsymbol{v}_i) - \sum_i \boldsymbol{r}_i \left(\sum_{m=2}^{4} \sum_{\phi \in \mathbb{P}_{mi}} \frac{1}{m} \sum_{j \in \phi} \boldsymbol{F}_{j\phi} \cdot \boldsymbol{v}_j\right) \\
&= \sum_i \boldsymbol{r}_i \sum_{m=2}^{4} \sum_{\phi \in \mathbb{P}_{mi}} \left(\boldsymbol{F}_{i\phi} \cdot \boldsymbol{v}_i - \frac{1}{m} \sum_{j \in \phi} \boldsymbol{F}_{j\phi} \cdot \boldsymbol{v}_j\right) \\
&= \sum_{m=2}^{4} \sum_{\phi \in \mathbb{P}_m} \sum_{i \in \phi} \boldsymbol{r}_i \left(\boldsymbol{F}_{i\phi} \cdot \boldsymbol{v}_i - \frac{1}{m} \sum_{j \in \phi} \boldsymbol{F}_{j\phi} \cdot \boldsymbol{v}_j\right) \\
&= \sum_{m=2}^{4} \sum_{\phi \in \mathbb{P}_m} \left(\frac{1}{m} \sum_{i \in \phi} \sum_{j \in \phi} \boldsymbol{r}_i (\boldsymbol{F}_{i\phi} \cdot \boldsymbol{v}_i - \boldsymbol{F}_{j\phi} \cdot \boldsymbol{v}_j)\right) \\
&= \sum_{m=2}^{4} \sum_{\phi \in \mathbb{P}_m} \left(\frac{1}{m} \sum_{\{i,j\} \in [\phi]^2} \left[\boldsymbol{r}_i (\boldsymbol{F}_{i\phi} \cdot \boldsymbol{v}_i - \boldsymbol{F}_{j\phi} \cdot \boldsymbol{v}_j) + \boldsymbol{r}_j (\boldsymbol{F}_{j\phi} \cdot \boldsymbol{v}_j - \boldsymbol{F}_{i\phi} \cdot \boldsymbol{v}_i)\right]\right)
\end{aligned}$$

$$= \sum_{m=2}^{4} \sum_{\phi \in \mathbb{P}_m} \left(\frac{1}{m} \sum_{\{i,j\} \in [\phi]^2} \left[\boldsymbol{r}_{ij} \left(\boldsymbol{F}_{i\phi} \cdot \boldsymbol{v}_i - \boldsymbol{F}_{j\phi} \cdot \boldsymbol{v}_j \right) \right] \right) \quad (7abcdef)$$

We are able to incorporate the $\boldsymbol{F}_i \cdot \boldsymbol{v}_i$ term into the outer summations because the total force on i is equivalent to all the forces on i due to all m-body potentials ϕ, i.e. $\boldsymbol{F}_i = \sum_{m=2}^{4} \sum_{\phi \in \mathbb{P}_{mi}} \boldsymbol{F}_{i\phi} \cdot \boldsymbol{v}_i$. We are then able to invert the summations and sum across all atoms i in a potential ϕ for all potentials, rather than summing all potentials ϕ that atom i is part of. For the inner summation, if we sum $\boldsymbol{F}_{i\phi} \cdot \boldsymbol{v}_i$ m times (once for every j in the given m-body potential ϕ), then we would need to divide it by m, i.e. $\boldsymbol{F}_{i\phi} \cdot \boldsymbol{v}_i = \frac{1}{m} \sum_{j \, in \, \phi_{atoms}} \boldsymbol{F}_{i\phi} \cdot \boldsymbol{v}_i$. Finally, to use the relative positions $\boldsymbol{r}_{ij}$, we need to recognize that in equation 7d for every pair $\{i = i_1, j = j_1\}$, there will be a corresponding pair $\{i = j_1, j = i_1\}$ and we can sum them twice per pair if we replace the double sums across i and j with one sum across all pairs that make up the potential.

Our final general expression for the heat flux will therefore be:

$$\boldsymbol{J}V = \sum_i E_i \boldsymbol{v}_i + \sum_{m=2}^{4} \sum_{\phi \in \mathbb{P}_m} \left(\frac{1}{m} \sum_{\{i,j\} \in [\phi]^2} \left[\boldsymbol{r}_{ij} \left(\boldsymbol{F}_{i\phi} \cdot \boldsymbol{v}_i - \boldsymbol{F}_{j\phi} \cdot \boldsymbol{v}_j \right) \right] \right) \quad (8)$$

This is a per-potential version of the general heat flux, meaning we sum across the various potentials in the system, and then across all possible pairs of atoms included in the potential. The term inside the outermost parentheses is the heat flux for one specific m-body potential ϕ. To more easily compare to the virial stress heat flux in LAMMPS, we will also need a version of the heat flux that is rearranged to be per-atom, where we sum across all atoms and then across all potentials that include that atom. This rearrangement is straightforward; the only thing to note is that there is an extra factor of 2 due to the summations above being over the pairs $\{i, j\}$ and the one below being over all atoms i and then all $j \in \phi$, yielding two pairs $\{i = i_1, j = j_1\}$ and $\{i = j_1, j = i_1\}$:

$$\boldsymbol{J}V = \sum_i E_i \boldsymbol{v}_i + \sum_i \sum_{m=2}^{4} \frac{1}{2m} \sum_{\phi \in \mathbb{P}_{mi}} \sum_{j \in \phi} \left[\boldsymbol{r}_{ij} \left(\boldsymbol{F}_{i\phi} \cdot \boldsymbol{v}_i - \boldsymbol{F}_{j\phi} \cdot \boldsymbol{v}_j \right) \right] \quad (9)$$

We can now show that this equation, when limited to two-body potentials only, is equivalent to the Irving and Kirkwood and Hardy derivations:

$$\begin{aligned} (\boldsymbol{J}V)_{\mathbb{P}_2} &= \sum_i E_i \boldsymbol{v}_i + \sum_i \frac{1}{4} \sum_{\phi \in \mathbb{P}_{2i}} \sum_{j \in \phi} \left[\boldsymbol{r}_{ij} \left(\boldsymbol{F}_{i\phi} \cdot \boldsymbol{v}_i - \boldsymbol{F}_{j\phi} \cdot \boldsymbol{v}_j \right) \right] \\ &= \sum_i E_i \boldsymbol{v}_i + \sum_i \frac{1}{4} \sum_{\phi \in \mathbb{P}_{2i}} \sum_{j \, \in \, \phi \backslash \{i\}} \left[\boldsymbol{r}_{ij} \left(\boldsymbol{F}_{i\phi} \cdot \left(\boldsymbol{v}_i + \boldsymbol{v}_j \right) \right) \right] \\ &= \sum_i E_i \boldsymbol{v}_i + \frac{1}{2} \sum_i \sum_{j>i} \left[\boldsymbol{r}_{ij} \left(\boldsymbol{F}_{ij} \cdot \left(\boldsymbol{v}_i + \boldsymbol{v}_j \right) \right) \right] \end{aligned} \quad (10abc)$$

For a two-body potential, there will be only two j's for each ϕ; one of them will be equal to i and can be omitted. Then the summations $\sum_{\phi \in \mathbb{P}_{2i}} \sum_{j \in \phi}$ can be replaced with the simpler summations $\sum_i \sum_{j>i}$ as long as one also replaces the force term, $\boldsymbol{F}_{i\phi} = \boldsymbol{F}_{ij,\phi}$ and $\boldsymbol{F}_{ij} = \sum_\phi \boldsymbol{F}_{ij,\phi}$. This final equation 10c is recognizable as Irving and Kirkwood's definition of the molecular interaction component of the heat flux for a uniform system in absence of fluid flow.[16] Further, equation 10c is also identical to Hardy's definition of the potential component for heat flux, also for a uniform system in absence of fluid flow[17].

Continuing with the assumption that there are only two-body potentials defined on the system, we can now derive the LAMMPS virial stress tensor heat flux, starting with showing how a general definition of the stress tensor relates to the per-atom version that LAMMPS uses. The global stress tensor $\boldsymbol{S}$ is defined to be the ensemble average of a kinetic term summed across all N atoms in the system and the virial tensor,[19] (or stress) $\boldsymbol{W}(\boldsymbol{r}^N)$, which is a function of the N positions $\boldsymbol{r}^N$,

$$\boldsymbol{S}V = \langle \sum_{i=1}^{N} m_i \boldsymbol{v}_i \boldsymbol{v}_i + \boldsymbol{W}(\boldsymbol{r}^N) \rangle \tag{11}$$

where V is the volume, and m_i and v_i are the mass and velocity of atom i. When calculating heat flux, LAMMPS excludes the kinetic term, leaving just the ensemble average of the virial stress. We can expand the virial term using the positions $\boldsymbol{r}_i$ and the total force $\boldsymbol{F}_i$ on atom i:

$$\langle \boldsymbol{W}(\boldsymbol{r}^N) \rangle = \langle \sum_i \boldsymbol{r}_i \boldsymbol{F}_i \rangle \tag{12}$$

We can further break this up by recognizing that $\boldsymbol{F}_i$ will be a summation of the forces caused by all the potentials defined in the system:

$$\langle \boldsymbol{W}(\boldsymbol{r}^N) \rangle = \langle \sum_i \sum_{\phi \in \mathbb{P}_{2i}} \boldsymbol{r}_i \boldsymbol{F}_{i\phi} + \sum_i \sum_{\phi \in \mathbb{P}_{3i}} \boldsymbol{r}_i \boldsymbol{F}_{i\phi} + \sum_i \sum_{\phi \in \mathbb{P}_{4i}} \boldsymbol{r}_i \boldsymbol{F}_{i\phi} \rangle = \langle \sum_i \sum_{m=2}^{4} \sum_{\phi \in \mathbb{P}_{mi}} \boldsymbol{r}_i \boldsymbol{F}_{i\phi} \rangle \tag{13}$$

To get the per-atom form of the virial stress tensor that LAMMPS uses to calculate the heat flux, we separate the ensemble average of the virial stress into contributions from each atom, which LAMMPS calls a "per-atom stress tensor" and denoted here by $\boldsymbol{s}_i$:

$$\langle \boldsymbol{W}(\boldsymbol{r}^N) \rangle = \langle \sum_i \boldsymbol{s}_i \rangle \tag{14}$$

where

$$\boldsymbol{s}_i = \sum_{m=2}^{4} \sum_{\phi \in \mathbb{P}_{mi}} \frac{1}{m} \sum_{j \in \phi} \boldsymbol{r}_j \boldsymbol{F}_{j\phi} \tag{15}$$

Equation 13 is equivalent to equations 14-15. In the former, the virial terms $\boldsymbol{r}_i \boldsymbol{F}_{i\phi}$ are summed once per atom / potential pair. In the latter, the virial terms $\boldsymbol{r}_j \boldsymbol{F}_{j\phi}$ are summed up by potential so each term will appear m times, once for every atom j in the potential ϕ; the sum of the virial terms is then divided amongst the potential's constituent atoms. As mentioned above, the potential could be divided amongst the atoms in a different manner, but LAMMPS chooses to divide the potential evenly.

LAMMPS defines the instantaneous heat flux $\boldsymbol{J}$ as:[14]

$$(\boldsymbol{J}V)_{LAMMPS} = \sum_i E_i \boldsymbol{v}_i - \sum_i \boldsymbol{s}_i \cdot \boldsymbol{v}_i \tag{16}$$

The $\boldsymbol{J}_{cnv}$ term $\sum_i E_i \boldsymbol{v}_i$ is equivalent to our derivation (equations 8-9) so we can focus on showing equivalence for just the $\boldsymbol{J}_{pot}$ term. Starting with the $\boldsymbol{J}_{pot}$ term from our general expression (equation 9), and limiting it to two body potentials, we can tie it out to the $\boldsymbol{J}_{pot}$ of the per-atom virial stress heat flux used in LAMMPS:

$$\begin{aligned}
\boldsymbol{J}_{pot,\mathbb{P}_2} &= \sum_i \frac{1}{4} \sum_{\phi \in \mathbb{P}_{2i}} \sum_{j \in \phi \setminus \{i\}} \boldsymbol{r}_{ij} \left(\boldsymbol{F}_{i\phi} \cdot \left(\boldsymbol{v}_i + \boldsymbol{v}_j \right) \right) \\
&= \sum_i \frac{1}{4} \sum_{\phi \in \mathbb{P}_{2i}} \sum_{j \in \phi \setminus \{i\}} \left[\left(\boldsymbol{r}_{ij} \boldsymbol{F}_{i\phi} \right) \cdot \boldsymbol{v}_i + \left(\boldsymbol{r}_{ij} \boldsymbol{F}_{i\phi} \right) \cdot \boldsymbol{v}_j \right] \\
&= \sum_i \frac{1}{4} \sum_{\phi \in \mathbb{P}_{2i}} \sum_{j \in \phi \setminus \{i\}} \left[\left(\boldsymbol{r}_{ij} \boldsymbol{F}_{i\phi} \right) \cdot \boldsymbol{v}_i + \left(\boldsymbol{r}_{ji} \boldsymbol{F}_{j\phi} \right) \cdot \boldsymbol{v}_j \right] \\
&= \sum_i \frac{1}{2} \sum_{\phi \in \mathbb{P}_{2i}} \sum_{j \in \phi \setminus \{i\}} \left(\boldsymbol{r}_{ij} \boldsymbol{F}_{i\phi} \right) \cdot \boldsymbol{v}_i \\
&= \sum_i \frac{1}{2} \sum_{\phi \in \mathbb{P}_{2i}} \sum_{j \in \phi \setminus \{i\}} \left(\boldsymbol{r}_i \boldsymbol{F}_{i\phi} + \boldsymbol{r}_j \boldsymbol{F}_{j\phi} \right) \cdot \boldsymbol{v}_i \\
&= \sum_i \frac{1}{2} \left[\sum_{\phi \in \mathbb{P}_{2i}} \sum_{j \in \phi} \boldsymbol{r}_j \boldsymbol{F}_{j\phi} \right] \cdot \boldsymbol{v}_i \\
&= \sum_i \left[\boldsymbol{s}_i \right]_{\phi \in \mathbb{P}_{2i}} \cdot \boldsymbol{v}_i
\end{aligned} \tag{17abcdefg}$$

Hence, equation 9, limited to two-body potentials, is equivalent to the LAMMPS heat flux definition, also limited to two-body potentials. This shows that LAMMPS's use of the virial stress tensor form of the heat flux is justified, when limited to two-body potentials.

LAMMPS, however, extends this virial stress beyond two-body potentials to three- and four-body potentials by making the leap that because virial stress can describe the heat flux for two-body potentials, then it can also describe the heat flux for three- and four-body potentials, i.e., if $\boldsymbol{J}_{pot,\mathbb{P}_2} = \sum_i [\boldsymbol{s}_i]_{\phi \in \mathbb{P}_{2i}} \cdot \boldsymbol{v}_i$, then $\boldsymbol{J}_{pot,\mathbb{P}} = \sum_i [\boldsymbol{s}_i]_{\phi \in \mathbb{P}} \cdot \boldsymbol{v}_i$. This step is not valid. It may be easier to see the difference between the virial stress heat flux and the correct heat flux when comparing the heat flux contribution between the two forms for only one three-body potential $\phi = \{a, b, c\} \in \mathbb{P}_3$. The correct heat flux, starting from equation (8), will be:

$$\begin{aligned}
\boldsymbol{J}_{pot,\phi=\{a,b,c\}} &= \left[\frac{1}{m} \sum_{\{i,j\} \in [\phi]^2} \boldsymbol{r}_{ij} \left(\boldsymbol{F}_{i\phi} \cdot \boldsymbol{v}_i - \boldsymbol{F}_{j\phi} \cdot \boldsymbol{v}_j \right) \right]_{\phi=\{a,b,c\}} \\
&= \frac{1}{3} \left[\boldsymbol{r}_{ab} \left(\boldsymbol{F}_{a\phi} \cdot \boldsymbol{v}_a - \boldsymbol{F}_{b\phi} \cdot \boldsymbol{v}_b \right) + \boldsymbol{r}_{bc} \left(\boldsymbol{F}_{b\phi} \cdot \boldsymbol{v}_b - \boldsymbol{F}_{c\phi} \cdot \boldsymbol{v}_c \right) + \boldsymbol{r}_{ac} \left(\boldsymbol{F}_{a\phi} \cdot \boldsymbol{v}_a - \boldsymbol{F}_{c\phi} \cdot \boldsymbol{v}_c \right) \right] \\
&= \frac{1}{3} \left[(\boldsymbol{r}_{ab} + \boldsymbol{r}_{ac}) (\boldsymbol{F}_{a\phi} \cdot \boldsymbol{v}_a) + (\boldsymbol{r}_{bc} - \boldsymbol{r}_{ab}) (\boldsymbol{F}_{b\phi} \cdot \boldsymbol{v}_b) + (-\boldsymbol{r}_{bc} - \boldsymbol{r}_{ac}) (\boldsymbol{F}_{c\phi} \cdot \boldsymbol{v}_c) \right] \\
&= \frac{1}{3} \left[\left[(\boldsymbol{r}_{ab} + \boldsymbol{r}_{ac}) \boldsymbol{F}_{a\phi} \right] \cdot \boldsymbol{v}_a + \left[(\boldsymbol{r}_{bc} - \boldsymbol{r}_{ab}) \boldsymbol{F}_{b\phi} \right] \cdot \boldsymbol{v}_b + \left[(-\boldsymbol{r}_{bc} - \boldsymbol{r}_{ac}) \boldsymbol{F}_{c\phi} \right] \cdot \boldsymbol{v}_c \right]
\end{aligned} \tag{18abcd}$$

Whereas the virial stress heat flux for one three-body potential $\phi = \{a, b, c\} \in \mathbb{P}_3$, starting with equations 15-16:

$$\begin{aligned}
\boldsymbol{J}_{pot,\phi\in\{a,b,c\}} &= \left[\sum_i [\boldsymbol{s}_i]_\phi \cdot \boldsymbol{v}_i\right]_{\phi=\{a,b,c\}} \\
&= \left[\sum_{i\in\phi} \frac{1}{3}\left(\sum_{j\in\phi} \boldsymbol{r}_j \boldsymbol{F}_{j\phi}\right) \cdot \boldsymbol{v}_i\right]_{\phi=\{a,b,c\}} \\
&= \frac{1}{3}\left(\boldsymbol{r}_a \boldsymbol{F}_{a\phi} + \boldsymbol{r}_b \boldsymbol{F}_{b\phi} + \boldsymbol{r}_c \boldsymbol{F}_{c\phi}\right) \cdot (\boldsymbol{v}_a + \boldsymbol{v}_b + \boldsymbol{v}_c) \\
&= \frac{1}{3}\left(\boldsymbol{r}_{ab} \boldsymbol{F}_{a\phi} + \boldsymbol{r}_{ca} \boldsymbol{F}_{c\phi}\right) \cdot (\boldsymbol{v}_a + \boldsymbol{v}_b + \boldsymbol{v}_c) \qquad (19abcd)
\end{aligned}$$

For the virial stress heat flux, the virial stress term is the same for all atoms in the potential; this can therefore be multiplied by the sum of the velocities. For the correct form of the heat flux, however, the terms that multiply the atom velocities are all different from one another and cannot be combined. Curious readers can see the implementation of equation 19 by looking at the referenced LAMMPS source code files[20,21].

As shown above, the virial stress heat flux that LAMMPS uses is valid for two body potentials; however, the virial stress heat flux cannot be extended to three- and four-body potentials which may lead to erroneous thermal conductivity predictions. We suspect that the reason why this problem has mostly gone unnoticed is because for many systems, the amount of heat flux being transferred via the three- or four-body potentials is diminutive, so that any error due to the calculation of heat flux for those potentials is rendered largely inconsequential. The error may also be further obscured by compensating factors when using the heat flux for the purpose of calculating thermal conductivity via Green-Kubo. Comparisons of the corrected and virial stress heat flux calculations in example systems follow in the results section.

Notes on Implementation in LAMMPS

The error described above applies to all many-body potentials in LAMMPS. However, in LAMMPS, there are two different categories of many-body potentials and these different categories require separate code fixes. These two different categories are (1) many-body potentials defined on sets of three or more atoms where the sets are defined in advance, usually due to the bonding structure (i.e., the angle, dihedral, and improper styles in LAMMPS), and (2) many-body potentials where the atoms that interact change over the course of the simulation (i.e. potentials implemented via the unfortunately named "pair potential" style such as the Tersoff, Brenner, and Stillinger-Weber potentials, and the AGNI and GAP machine learning potentials). The code fix that we have implemented addresses the first category of potentials only. Other research groups are working on the second category of potentials.[15]

Due to how LAMMPS stores atoms across multiple processors, the velocity for an atom can only be found on the processor the atom is assigned to. In order to support this, rather than dividing the heat flux evenly between the atoms that comprise the potential, we assign the portion of the heat flux that contains the velocity of an atom to that atom. For a single three-body potential $\phi = \{a, b, c\}$, the heat fluxes assigned to the atoms a, b, c will be:

$$\begin{aligned}
(\boldsymbol{JV})_{\phi,a} &= \frac{1}{3}\left[(\boldsymbol{r}_{ab} + \boldsymbol{r}_{ac})\boldsymbol{F}_{a\phi}\right] \cdot \boldsymbol{v}_a \\
(\boldsymbol{JV})_{\phi,b} &= \frac{1}{3}\left[(\boldsymbol{r}_{bc} - \boldsymbol{r}_{ab})\boldsymbol{F}_{b\phi}\right] \cdot \boldsymbol{v}_b \\
(\boldsymbol{JV})_{\phi,c} &= \frac{1}{3}\left[(-\boldsymbol{r}_{bc} - \boldsymbol{r}_{ac})\boldsymbol{F}_{c\phi}\right] \cdot \boldsymbol{v}_c \qquad (20abc)
\end{aligned}$$

These equations are just the individual terms in equation (18d). The total heat flux assigned is unchanged; the only difference is that the velocity the atom a is now only used in the calculation of the heat flux on atom a, and so forth with the velocities and heat fluxes for atoms b and c. Dividing the heat flux in this manner guarantees us the ability to calculate the heat flux, regardless of boundary conditions and number of processors.

We implemented the corrected algorithm described above for angle, dihedral and improper potential styles and it is currently available via our GitHub page at https://github.com/wilmerlab/lammps.

Results and Discussion

For the example systems, we combined a typical non-equilibrium molecular dynamics (NEMD) setup–we enforced a heat flux by adding and removing a fixed amount of energy from two regions–with measurements of the heat flux using the corrected heat flux or the uncorrected LAMMPS virial stress heat flux. The procedure was: a rectangular cuboid simulation box with periodic boundaries was filled with a crystalline solid or a liquid, and after an initial equilibration, we ran an NVE simulation with a fixed heat source applied to the center of the cuboid and a corresponding sink applied to the outer edges (see Figure 1a). After the temperature profiles reached steady-state, we recorded the instantaneous heat fluxes for control volumes on the left and right sides of the box, and averaged them over a time-frame necessary for convergence.

The instantaneous heat fluxes were recorded separately for the convective heat flux as well as any defined pair, bond, angle, dihedral, and improper potentials using both the corrected and uncorrected LAMMPS code. Because we are using the NVE ensemble, and the heat added and removed is fixed, the heat flux code should self-consistently report the applied heat flux, regardless of the force-field parameters, and we can therefore use this as an accurate gauge of measuring the correctness of our implementation. We have included our simulation parameters

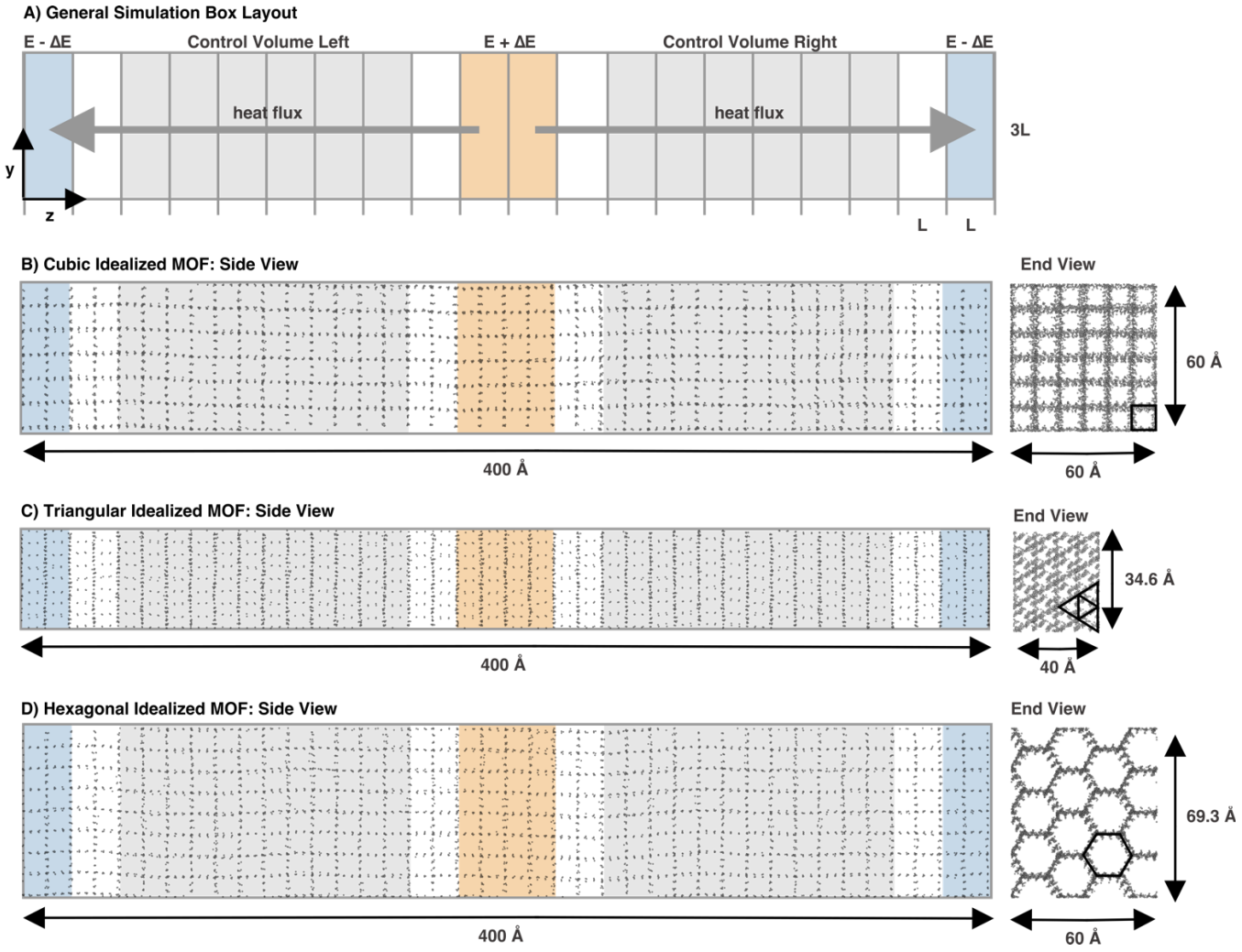

Figure 1: (A) Side view of the layout of a simulation box, where the box is broken up into slabs of width and height 3L and depth L. Energy is added to the two center slabs (in orange) at the rate of ΔE per slab and removed from the two end slabs (in blue) at the same rate. The heat flux is measured in the two control regions (in grey). (B),(C), and (D) are snapshots of the cubic, triangular and hexagonal idealized MOFs with both side and end views

below for completeness, but in all cases, the calculated heat flux should be a function of the applied energy and the control volume size alone.

For this simulation setup, the corrected total instantaneous heat flux calculation does not require steady-state to be reached; the recorded instantaneous heat flux may be averaged immediately upon application of the heat source (see Figure 6). This is in contrast to the per-potential averages, which took a significant amount of time to converge after steady-state, from between 40-215M timesteps. Calculating the per-potential heat fluxes is usually unnecessary unless one is studying the distribution of heat flux between different potentials (or writing software to fix it); researchers should not take the number of timesteps required for our simulations to be indicative of the number required to measure the total heat flux.

Example System 1: Idealized MOF structures

For testing the 3-body potential, we examined cubic, triangular and hexagonal idealized metal-organic framework (MOF) structures (see Figure 1(B)(C)(D)); a full description of these idealized MOF structures, including force field parameters, is covered in a previous paper[22] and we will present only the briefest description here. These idealized structures are simplified models corresponding to common actual geometries of real MOFs; a simple geometric shape is extended orthogonally to the plane of the shape in a series of channels, forming a lattice that stretches over the whole cuboid and connects across the periodic boundaries. The force field is defined with only bond and angle potentials, with parameters chosen to approximate the thermal conductivity of a typical MOF. After relaxation of the system using NVT / NVE for 500,000 timesteps, an energy source and sink was applied of 0.0040 kcal / mol fs for the cubic structure, 0.0071 kcal / mol fs for the triangular structure, and 0.0213 kcal / mol fs for the hexagonal structure. After a steady-state was reached at 5M timesteps, the per potential heat flux was averaged over 15M timesteps.

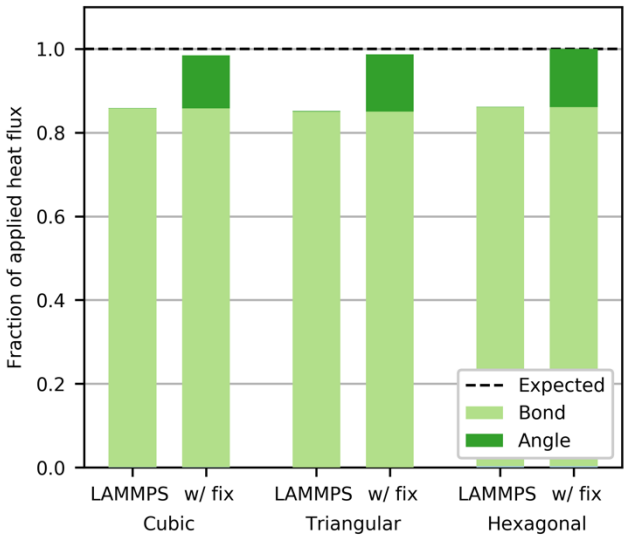

Figure 2: Per-potential fraction of applied heat flux for both uncorrected LAMMPS and corrected calculations for idealized cubic, triangular and hexagonal MOFs.

Because the lattice has zero aggregate momentum, there should be negligible heat transport through convection and all of the heat flux should travel through the bond and angle potentials. As measured for all three systems, the summation of the bond and angle heat fluxes from the corrected code equals the expected heat flux as calculated from the applied energy (see Figure 2). The uncorrected LAMMPS code shows nearly zero heat flux through the angle potential and the error of the total flux is equivalent to the missing angle potential, or about 15% of the expected total flux.

Example System 2: Propane, Octane and Hexadecane

To demonstrate the corrected 3- and 4-body potentials work in conjunction to correctly predict heat flux in a real-life system, we ran simulations for propane, octane and hexadecane. Simulation parameters were adapted from Ohara, et al[23] in order to compare directly with their per-potential results; a brief description of the parameters follows. Each hydrocarbon was defined using the united atom NERD force field[24] and packed into the rectangular cuboid simulation box using Packmol[25] to the density expected at a temperature of 0.7 times the critical temperature (see Figure 3). The simulation box was set to be 3L x 3L x 20L, where L is a hydrocarbon-specific length equal to 1/3 of the total of the length of the hydrocarbon + a buffer of 3 Å + the Lennard-Jones cutoff of 13.8 Å defined by the NERD forcefield. For propane, octane and hexadecane, 3L = 19.38 Å, 25.84 Å, and 36.17 Å, respectively. A timestep of 1 fs was used for all simulations. The system was equilibrated using NVT/NVE for 5M total timesteps; this larger-than-typical equilibration time is because we wanted a longer baseline for statistical averaging for comparing heat flux measurements before and after the application of a heat flux. After equilibration, an energy source and sink were applied of 9.4E-04 kcal / mole for propane, 8.3E-04 kcal / mole fs for octane, and 6.5E-04 kcal / mole fs for hexadecane in order to get an appropriate temperature profile. After 10M timesteps, stable temperature profiles were obtained and then heat flux data was recorded and averaged over 64M timesteps for propane, 132M timesteps for octane, and 234M timesteps for hexadecane.

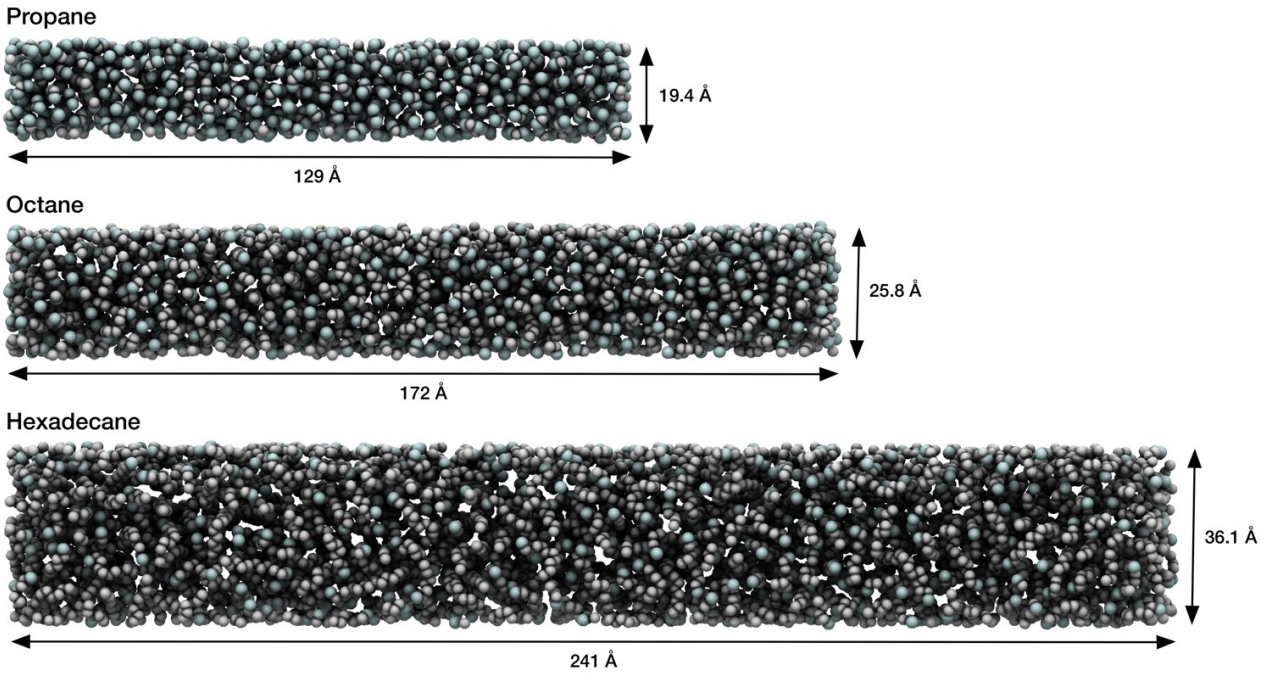

Figure 3: Simulation box layout for propane, octane and hexadecane.

Similar to the case of the idealized MOFs, the summation of all the terms in the corrected heat flux code approximately equals the expected heat flux, regardless of the length of the hydrocarbon (see Figure 4).

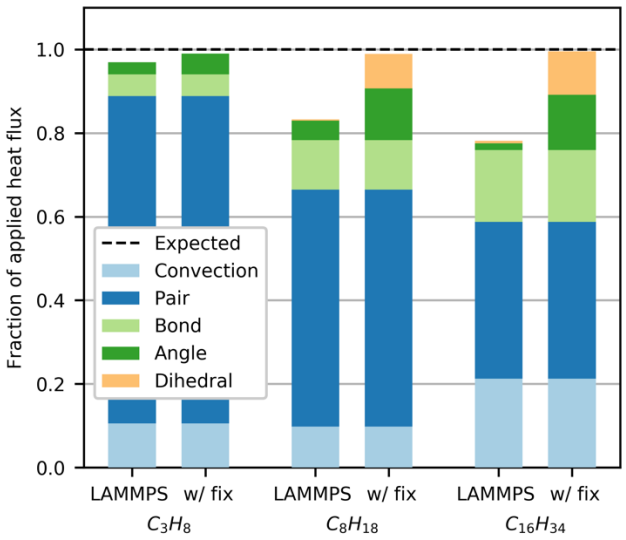

Figure 4: Per-potential fraction of applied heat flux for both uncorrected LAMMPS and corrected calculations for various hydrocarbons. As the length of the hydrocarbon increases, the heat transfer through the many-body potentials increases. $C_{16}H_{34}$ shows LAMMPS-reported heat fluxes of near zero for the angle and dihedral potentials, causing a total error of about 22%.

For the uncorrected code, as the length of the hydrocarbon increases, the amount of heat transfer through the angle and dihedral potentials increases, leading to greater errors with longer hydrocarbons. For propane, the error is minimal, but for octane, the error is greater than 16% and for hexadecane the error reaches 22%. This compares well to the results of Ohara, et al,[23] which roughly predict increasing dependence on the many-body potentials with increasing hydrocarbon length (see Figure 5). A comparable simulation of octane using improper potentials in place of dihedral potentials was also performed; the improper results were comparable to the dihedral results (see Supporting Information).

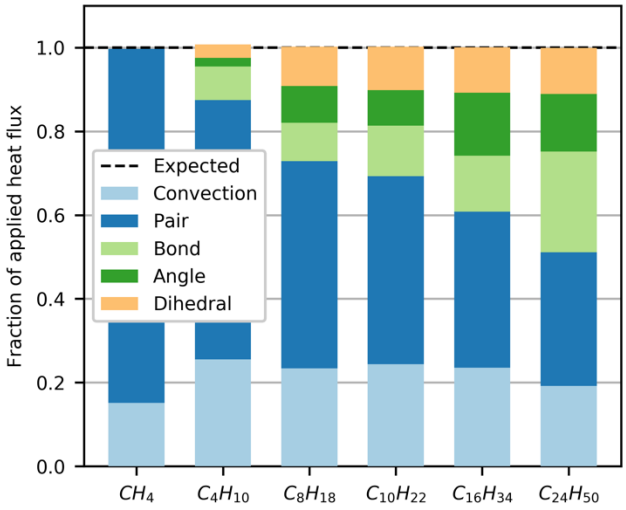

Figure 5. Per-potential fraction of applied heat flux for hydrocarbons from Ohara, et al, which predict increasing reliance on the angle and dihedral many-body terms for heat flux transfer with increasing hydrocarbon length.

In addition to the total error of 16% recorded for octane, the heat flux predicted by uncorrected LAMMPS shows greater swings in magnitude and visually doesn't converge as clearly (see Figure 6).

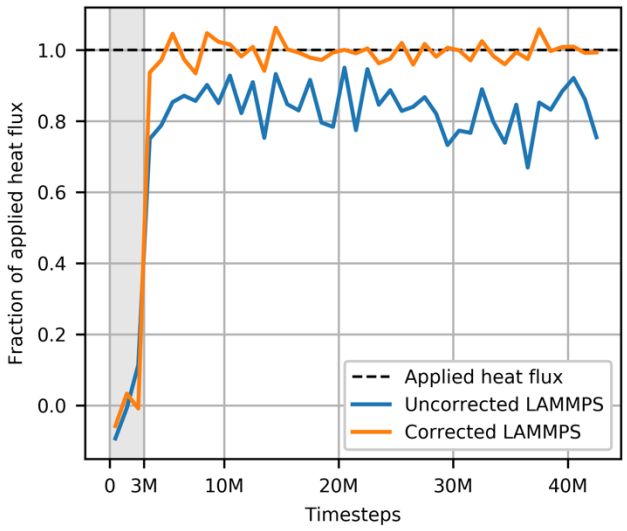

Figure 6: Total heat flux as a fraction of applied heat flux for both the uncorrected LAMMPS calculation (blue) and the corrected LAMMPS calculation (orange), averaged over 1M timesteps, as measured on octane. Prior to 3M timesteps, there is no applied heat flux (noted in grey) and the recorded instantaneous heat flux fluctuates around zero; after 3M timesteps, the heat flux is applied and the corrected calculation fluctuates around the correct value but the uncorrected calculation underestimates the real value as well as shows greater magnitude fluctuations

Any error in the long-term average of the heat flux, or any error that decorrelates the instantaneous heat flux may have consequences when calculating thermal conductivity via Green-Kubo; more research needs to be done to assess which systems are significantly affected by this error in the heat flux calculations.

Conclusion

For systems where significant heat transfer occurs within many-body potentials, the error in the uncorrected LAMMPS heat flux code can reach nearly 100% of the many-body potential heat flux, which leads to an erroneous total heat flux calculation. From our example systems, the largest error in the total heat flux we saw was 22%, though it is not hard to imagine a system where more heat is transferred via the many-body potentials; in that case, the error would be expected to be proportionally higher. Care should be exercised when evaluating prior results to ensure thermal conductivity calculations are not erroneous due to the incorrectly defined heat flux. We have implemented the corrected algorithm into LAMMPS which extends the accuracy of heat flux measurements in LAMMPS to the 3- and 4-body potentials.

For deciding whether it is necessary to adopt the corrected code for your calculations, we recommend evaluating which one of these three cases your work fits into: (1) if you are modeling a system composed of only 2-body potentials, you can use the uncorrected LAMMPS heat flux calculation safely; (2) if you are modeling a system that uses 3- or 4-body potentials implemented via the angle, dihedral or improper potential styles, we recommend you adopt our corrected LAMMPS code available at https://github.com/wilmerlab/lammps; and (3) if you are modeling a system with any other many-body potentials, you will need to evaluate whether the potentials have correct or incorrect implementations of the instantaneous heat flux.

Acknowledgements

H.B. and C.E.W. gratefully acknowledge support from the National Science Foundation (NSF), award CBET- 1804011. We would like to acknowledge Alan J. H. McGaughey for the helpful discussions and early feedback. This research was supported in part by the University of Pittsburgh Center for Research Computing through the resources provided. Figures were primarily created using Python and Matplotlib,[26] Simulation snapshots were rendered with Avogadro 2.[27]

Supporting Information

Supporting information and results: definition of improper potentials in LAMMPS, CVFF and OPLS potential discussion, plot of per-potential fraction of applied heat flux for both uncorrected and corrected LAMMPS calculations for octane using dihedral and improper potentials.

Bibliography

(1) Torii, D.; Nakano, T.; Ohara, T. Contribution of Inter- and Intramolecular Energy Transfers to Heat Conduction in Liquids. *J. Chem. Phys.* **2008**, *128*, 044504.

(2) Plimpton, S. Fast Parallel Algorithms for Short-Range Molecular Dynamics. *J. Comput. Phys.* **1995**, *117*, 1–19.

(3) Sezginel, K. B.; Asinger, P. A.; Babaei, H.; Wilmer, C. E. Thermal Transport in Interpenetrated Metal–Organic Frameworks. *Chem. Mater.* **2018**, *30*, 2281–2286.

(4) Henry, A.; Chen, G. High Thermal Conductivity of Single Polyethylene Chains Using Molecular Dynamics Simulations. *Phys. Rev. Lett.* **2008**, *101*, 235502.

(5) Xu, X.; Pereira, L. F. C.; Wang, Y.; Wu, J.; Zhang, K.; Zhao, X.; Bae, S.; Tinh Bui, C.; Xie, R.; Thong, J. T. L.; et al. Length-Dependent Thermal Conductivity in Suspended Single-Layer Graphene. *Nat. Commun.* **2014**, *5*, 3689.

(6) Lv, W.; Henry, A. Phonon Transport in Amorphous Carbon Using Green – Kubo Modal Analysis. *Appl. Phys. Lett.* **2016**, *108*, 181905.

(7) Shiomi, J. Nonequilirium Molecular Dynamics Methods for Lattice Heat Conduction Calculations. *Annu. Rev. Heat Transf.* **2014**, *17*, 177–203.

(8) Schelling, P. K.; Phillpot, S. R.; Keblinski, P. Comparison of Atomic-Level Simulation Methods for Computing Thermal Conductivity. *Phys. Rev. B* **2002**, *65*, 144306.

(9) Müller-Plathe, F. A Simple Nonequilibrium Molecular Dynamics Method for Calculating the Thermal Conductivity. *J. Chem. Phys.* **1997**, *106*, 6082–6085.

(10) Kubo, R. Statistical-Mechanical Theory of Irreversible Processes. I. General Theory and Simple Applications to Magnetic and Conduction Problems. *J. Phys. Soc. Jpn.* **1957**, *12*, 570–586.

(11) Green, M. S. Markoff Random Processes and the Statistical Mechanics of Time-Dependent Phenomena. II. Irreversible Processes in Fluids. *J. Chem. Phys.* **1954**, *22*, 398–413.

(12) Ohara, T.; Chia Yuan, T.; Torii, D.; Kikugawa, G.; Kosugi, N. Heat Conduction in Chain Polymer Liquids: Molecular Dynamics Study on the Contributions of Inter- and Intramolecular Energy Transfer. *J. Chem. Phys.* **2011**, *135*, 034507.

(13) Rashidi, V.; Coyle, E. J.; Sebeck, K.; Kieffer, J.; Pipe, K. P. Thermal Conductance in Cross-Linked Polymers: Effects of Non-Bonding Interactions. *J. Phys. Chem. B* **2017**, *121*, 4600–4609.

(14) compute heat/flux command — LAMMPS documentation http://lammps.sandia.gov/doc/compute_heat_flux.html (accessed Feb 13, 2018).

(15) Fan, Z.; Pereira, L. F. C.; Wang, H.-Q.; Zheng, J.-C.; Donadio, D.; Harju, A. Force and Heat Current Formulas for Many-Body Potentials in Molecular Dynamics Simulations with Applications to Thermal Conductivity Calculations. *Phys. Rev. B* **2015**, *92*, 094301.

(16) Irving, J. H.; Kirkwood, J. G. The Statistical Mechanical Theory of Transport Processes. IV. The Equations of Hydrodynamics. *J. Chem. Phys.* **1950**, *18*, 817–829.

(17) Hardy, R. J. Formulas for Determining Local Properties in Molecular-dynamics Simulations: Shock Waves. *J. Chem. Phys.* **1982**, *76*, 622–628.

(18) McGaughey, A. J. H.; Kaviany, M. Phonon Transport in Molecular Dynamics Simulations: Formulation and Thermal Conductivity Prediction. In *Advances in Heat Transfer*; Greene, G. A., Hartnett†, J. P., Bar-Cohen, A., Cho, Y. I., Eds.; Elsevier, 2006; Vol. 39, pp 169–255.

(19) Thompson, A. P.; Plimpton, S. J.; Mattson, W. General Formulation of Pressure and Stress Tensor for Arbitrary Many-Body Interaction Potentials under Periodic Boundary Conditions. *J. Chem. Phys.* **2009**, *131*, 154107.

(20) lammps/compute_heat_flux.cpp at master · WilmerLab/lammps https://github.com/WilmerLab/lammps/blob/master/src/compute_heat_flux.cpp (accessed May 7, 2019).

(21) lammps/angle.cpp at master · WilmerLab/lammps https://github.com/WilmerLab/lammps/blob/master/src/angle.cpp (accessed May 7, 2019).

(22) Babaei, H.; McGaughey, A. J. H.; Wilmer, C. E. Effect of Pore Size and Shape on the Thermal Conductivity of Metal-Organic Frameworks. *Chem. Sci.* **2017**, *8*, 583–589.

(23) Ohara, T.; Chia Yuan, T.; Torii, D.; Kikugawa, G.; Kosugi, N. Heat Conduction in Chain Polymer Liquids: Molecular Dynamics Study on the Contributions of Inter- and Intramolecular Energy Transfer. *J. Chem. Phys.* **2011**, *135*, 034507.

(24) Nath, S. K.; Escobedo, F. A.; de Pablo, J. J. On the Simulation of Vapor–Liquid Equilibria for Alkanes. *J. Chem. Phys.* **1998**, *108*, 9905–9911.

(25) Martínez, L.; Andrade, R.; Birgin, E. G.; Martínez, J. M. PACKMOL: A Package for Building Initial Configurations for Molecular Dynamics Simulations. *J. Comput. Chem.* **2009**, *30*, 2157–2164.

(26) Hunter, J. D. Matplotlib: A 2D Graphics Environment. *Comput. Sci. Eng.* **2007**, *9*, 90–95.

(27) Hanwell, M. D.; Curtis, D. E.; Lonie, D. C.; Vandermeersch, T.; Zurek, E.; Hutchison, G. R. Avogadro: An Advanced Semantic Chemical Editor, Visualization, and Analysis Platform. *J. Cheminformatics* **2012**, *4*, 17.

TOC Graphic